



# NOVEL ULTRASTRUCTURE IN WATER- CONDUCTING CELLS OF THE LOWER DEVONIAN PLANT *SENNICAULIS HIPPOCREPIIFORMIS*

by P. KENRICK, D. EDWARDS and R. C. DALES

**ABSTRACT.** A description of the ultrastructure of the water-conducting cells in *Sennicaulis hippocrepiiformis* Edwards (1981), an early land plant of uncertain affinity, is based on pyrite and limonite permineralizations from two Lower Devonian localities in Dyfed and Powys, Wales. The ultrastructure of the two-layered cell wall is unique among land plants, although a simple large helical thickening suggests affinity with the Tracheophyta. The lumen of each cell is lined with a thin microporate layer that overlies the bulk of the wall, including the simple helical thickening, which has a spongy texture. Tapering end walls like those seen in tracheids have not been observed. The reconstruction of the cell wall is based on an analysis of the mineral and coalified material using polished thick sections and scanning electron microscopy; the interpretation relies on comparative morphology and recent advances in knowledge of the process of sedimentary pyrite formation. This novel cell type is shown to be very different from that recently described in a similarly preserved plant, *Gosslingia breconensis* Heard, and comparisons are also made with presumed water-conducting cells of other early land plants. The microporate layer resembles that found in some extant hepatics, although a convincing argument for a close phylogenetic relationship requires more information on the chemical structure of the wall layers and the morphology of the whole plant.

THE thirty-second annual address to the Palaeontological Association entitled 'Pioneering plants', while celebrating the variety in organization exhibited by early land plants, cautioned that preconceptions based on extant vegetation can impose restrictions on interpretation. The latter may be particularly important at a time of anatomical, biochemical and morphological innovation associated with the colonization of a new and highly stressful environment. Anticipation undoubtedly colours perception. An excellent example relates to the water-conducting tissues of land plants and, more specifically, to the tracheid or vessel which characterizes the vascular plant and which is essential to the homoiohydric condition.

Water-conducting cells of early land plant fossils have usually been interpreted as tracheids similar to those in extant plants. The presence of tracheids of apparently similar structure in different higher taxa (e.g. Rhyniophytina, Zosterophyllophytina, Trimerophytina and Lycophytina) has reinforced the concept of a monophyletic origin for these diverse groups. Recently, the identification and redescription of major cell wall features (e.g. thickening or pitting type) using scanning electron microscopy has shown that previous descriptions based on light microscope observations were often incorrect (Kenrick and Edwards 1988). Further technical refinement and a better understanding of how certain minerals form have also facilitated analysis and interpretation of cell wall ultrastructure. Thus detailed studies of the water-conducting cells ('tracheids') of the oldest well-preserved vascular plants have identified two distinctly different types of wall ultrastructure in cells that are superficially similar. The previously described *Gosslingia*-type (Kenrick and Edwards 1988) is comparable to protoxylem elements in some extant pteridophytes, whereas the *Sennicaulis*-type, described here, combines helical thickenings – a tracheid feature – with a thin microporate wall – a feature of the water-conducting cells of some hepatics.

## MATERIAL AND LOCALITIES

Three sets of sterile, permineralized axes showing similar wall structure were obtained from two localities in South Wales: Mill Bay West, a new locality in Dyfed, and Brecon Beacons Quarry in Powys. Most of the material illustrated here was collected from Mill Bay (Pl. 1, figs 1, 2, 6, 7; Pl. 2, figs 1–3, 6; Text-fig. 1A, B) and contains a high proportion of limonite (see p. 758). Two illustrations (Pl. 1, figs 3 and 4) are of pyritized material from the Edwards collection of *Sennicaulis hippocrepiiformis* from Brecon Beacons Quarry and now housed in the British Museum (Natural History) – BM(NH). This material contains little or no limonite and is a good example of the type of wall structure described here as seen in polished transverse section. Further limonitic material, collected from Brecon Beacons Quarry, is used to demonstrate the helical nature of the wall thickenings because it etched well (Pl. 1, figs 6 and 7). These two localities are in separate local units of the Lower Old Red Sandstone, namely the Cosheston Group and the Senni Beds (Allen 1974; Thomas 1978).

*Mill Bay West* (SN 002 049). This locality on the southern shore of the Daugleddau estuary, c. 3.5 km north-east of Pembroke Dock, is in the Mill Bay Formation (Thomas 1978) of the Cosheston Group. The sequence consists of dark, grey-green, highly indurated, c. 3 m thick, interlaminated very fine-grained sandstones and coarse siltstones which have been ‘pillowed’. The pillowing is thought to be of tectonic origin and has severely deformed the bedding planes. The locality, frequently submerged at high tide, is unit 269 of Thomas (1978) and is 126 m above the base of his MBW log D. The lithology is a difficult one from which to extract plants, but has yielded abundant, sterile, coalified axes with a central strand preserved in pyrite or limonite. These new fossils have been assigned to the form genus *Sennicaulis* based on anatomical observations of the central strand.

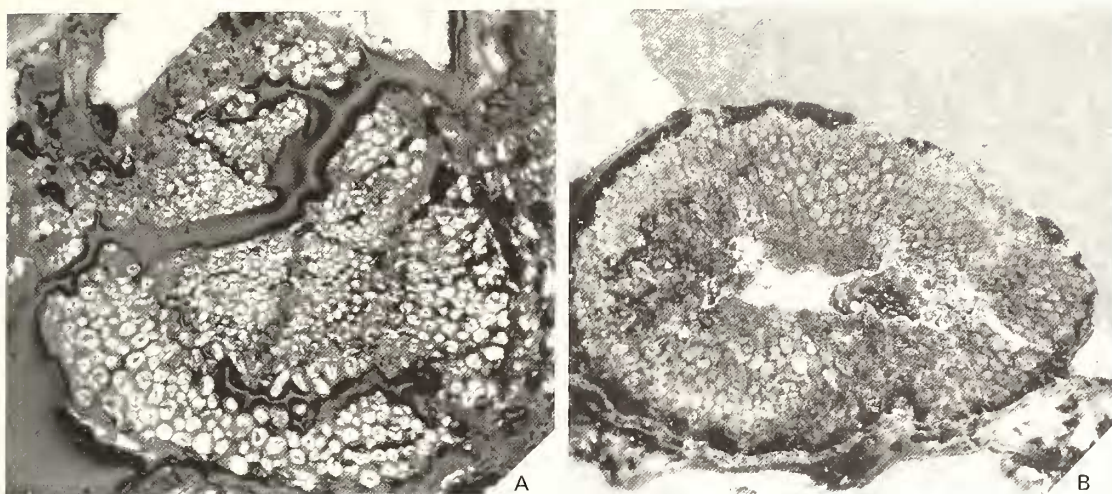
A comparative analysis of the lithostratigraphy and miospore assemblages of the Cosheston group and the Senni Beds led Thomas (1978) to equate the latter to the lower two-thirds of his Mill Bay Formation. This places the locality in the uppermost Gedinnian to lower Siegenian on palynological correlations (Richardson *et al.* 1982).

*Brecon Beacons Quarry* (SN 9715 2084). This is a disused roadside quarry c. 12 km south of Brecon on the main road (A470) to Merthyr Tydfil. About 14 m of the predominantly blue-grey fluvialite sediments of the Senni Beds are exposed. These consist of a series of massive sandstones (channel-fill deposits) which cut into and alternate with silty sandstones and siltstones. Some specimens assignable to *Sennicaulis*, and collected from the *Tarella trowenii* plant bed (Edwards and Kenrick 1986), contain significant amounts of limonite. One non-oxidized, pyritic specimen from the Edwards *Sennicaulis hippocrepiiformis* collection at the BM(NH) was examined. It was originally collected from plant bed 3, some 2 m above the main *Gosslingia* horizon (Friend and Williams 1978). The *Gosslingia breconensis* material illustrated here and first figured in Kenrick and Edwards (1988) was collected from horizon 4, the main *Gosslingia* plant bed (Friend and Williams 1978). Spore assemblages suggest a lowermost Siegenian age for both the *Tarella* and *Gosslingia* beds (lower part of Zone III, Richardson *et al.* 1982).

Figured specimens are housed in the National Museum of Wales, Cardiff (prefix NMW) or the British Museum (Natural History), London (prefix V).

## TECHNIQUES

Specimens were examined using incident light and scanning electron microscopy. Employing these two techniques in combination enables accurate reconstructions and interpretations of the cell wall of pyritic and limonitic fossils to be made. Incident light microscopy illustrates the distribution of mineral and coalified material within the wall which is essential for interpreting the electron



TEXT-FIG. 1. A, B, *Sennicaulis hippocrepiformis*; NMW 90.42G.1; Lower Old Red Sandstone; Mill Bay West, South Wales; transverse section of xylem strand at different levels along an axis,  $\times 70$ ; A, More or less terete strand composed of two zones of cells: inner zone of small cells surrounded by outer zone of large cells (specimen is cracked in upper left quarter). Pyrite in cell lumens (high reflectance), oxide in cell walls (low reflectance); B, elliptical shape to strand caused by collapse of outer zone cells into non-preserved middle region. Mineral is limonite.

micrographs. Scanning electron microscopy clearly illustrates the three-dimensional form of the cell and its ultrastructure.

For light microscopy, highly polished thick sections (Pl. 1; Text-fig. 1A) were made using a standard mineralogical polishing technique outlined in Kenrick and Edwards (1988). Bright field incident light microscopy produced the best results for pyritized axes and also for specimens with oxidized cell walls and pyritic lumens. Brief etching of the polished surface heightened contrast in pyritized specimens. The most effective etchant proved to be a saturated solution of ammonium ceric (IV) nitrate in dilute sulphuric acid (Biggs and Rocken 1983). The entirely limonitic specimen (Text-fig. 1B) was not polished, but saw marks were removed with 600 grit carborundum and the specimen mounted under a coverslip in Histomount and photographed using dark field illumination on an Olympus Vanox. A monochromatic green filter improved the photographic results obtained with Ilford PAN F or FP4 35 mm black-and-white film.

For scanning electron microscopy, a deep etch or a fractured surface was preferred. Concentrated solutions of nitric acid and hydrochloric acid were used to etch pyrite and limonite respectively. Etching time varied depending on the depth of etch required and the mineral present, but was typically between 5 and 15 minutes. In many instances, better results were obtained from fractured surfaces, which also served as a control for the effects of acids on wall structure in etched sections. All specimens were coated with gold and examined using a JEOL 35CS or Cambridge 360 scanning electron microscope.

#### SYSTEMATIC PALAEOLOGY

Edwards (1981) erected the genus *Sennicaulis* as a: 'Form genus for sterile axes, each with a prominent terete xylem strand lacking parenchyma, but for which surface characteristics and branching pattern are uncertain. Centrarch xylem composed of tracheids with annular and helical secondary thickenings surrounded by a zone of compressed thick-walled cells. Outer cortex consisting of several layers of elongate thick-walled cells. Inner cortex and epidermis not preserved.'



The specimen illustrated here (Text-fig. 1A, B) shows that the central region of these strands can be quite variable. The absence of a well-defined inner zone in Text-figure 1B, taken from the same axis as the section illustrated in Text-figure 1A, is probably due to poor preservation.

In her original description, Edwards interpreted the cell walls as being almost entirely replaced by pyrite, so no organic structure or ultrastructural features were described. Kenrick (1988) collected more material from Brecon Beacons Quarry and Mill Bay and described the wall structures illustrated here. Recently, Dales was able to confirm the presence of similar wall ultrastructure in material from the type collection. We propose, therefore, to emend the generic diagnosis, but our ignorance of the gross morphology of the plant precludes the use of any taxon above the generic level.

## INCERTAE SEDIS

### Genus SENNICAULIS Edwards (1981)

*Type species: Sennicaulis hippocrepeiformis* Edwards (1981).

*Original diagnosis.* See Edwards (1981, p. 225).

*Emended diagnosis.* Form genus for sterile axes  $\pm$  circular in cross section containing a prominent terete xylem strand but for which surface characteristics and branching pattern are unknown. Xylem composed of elongate elements with predominantly helical thickenings surrounding a terete central region of smaller cells. Xylem element wall two layered: a thin, continuous, microporate layer (next to cell lumen) covers a layer with spongy texture. Outer cortex consisting of several layers of elongate thick-walled cells. Inner cortex and epidermis not preserved.

### *Sennicaulis hippocrepeiformis* Edwards (1981)

Plate 1, figs 1–4, 6, 7; Plate 2, figs 1–6; Text-fig. 1A, B

1981 *Sennicaulis hippocrepeiformis* Edwards, p. 225, plates 1–6, figs 1–46.

*Holotype.* Sections V60352–V60386; figured in Edwards (1981) pl. 1, figs 1, 3, 6; pl. 2, figs 8, 12, 13; pl. 3, figs 15 and 16; pl. 4, fig. 24; pl. 5, figs 31, 33–36; pl. 6, figs 37–44.

*Paratypes.* Sections V60387–V60404 and V60405–V60429; figured in Edwards (1981) pl. 2, fig. 9; pl. 3, figs 17–22; pl. 4, figs 23, 25–28; pl. 5, figs 29, 30, 32; pl. 6, fig. 45.

*Type locality.* Brecon Beacons Quarry, Wales (Friend and Williams 1978), Lower Old Red Sandstone (= Siegenian), Lower Devonian.

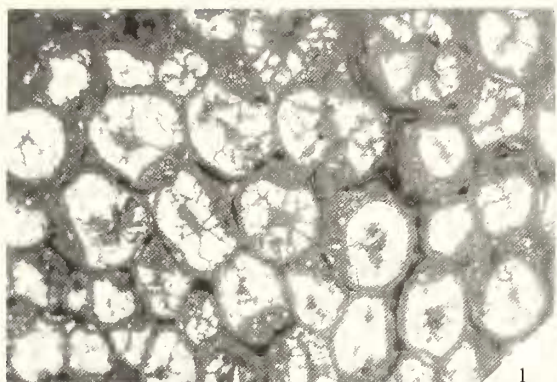
## EXPLANATION OF PLATE 1

Figs 1–4. *Sennicaulis hippocrepeiformis* Edwards; transverse sections (T.S.) of S-type conducting cells. 1 and 2, NMW 90.42G.1; Lower Old Red Sandstone; Mill Bay West, South Wales; outer and inner (respectively) zone cells, detail of Text-fig. 1A, pyrite cell lumina show high reflectance and limonitic cell walls low reflectance, thickenings arrowed,  $\times 315$ . 3 and 4, V 60388; Siegenian; Brecon Beacons Quarry, South Wales,  $\times 675$ .

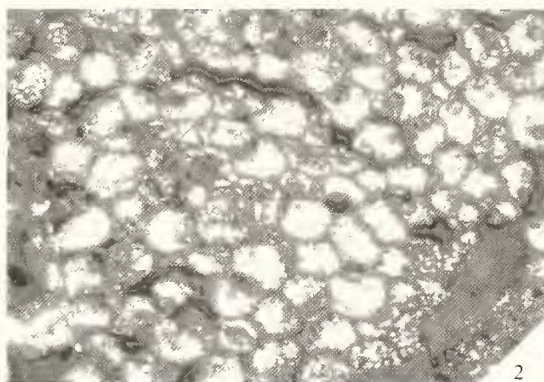
Fig. 5. *Gosslingia breconensis* (Kenrick and Edwards); NMW 87.19G.1; Siegenian; Brecon Beacons Quarry, South Wales; T.S. of G-type xylem cell,  $\times 675$ .

Figs 6 and 7. *S. hippocrepeiformis*; NMW 90.42G.2; Siegenian; Brecon Beacons Quarry, South Wales; longitudinal sections (L.S.) of S-type cells. 6, limonite. 7, pyrite in lumen, limonite in wall. Both  $\times 510$ .

Figs 8 and 9. *G. breconensis*; NMW 87.19G.2; Siegenian; Brecon Beacons Quarry, South Wales; L.S. of G-type cells preserved in pyrite,  $\times 510$ .



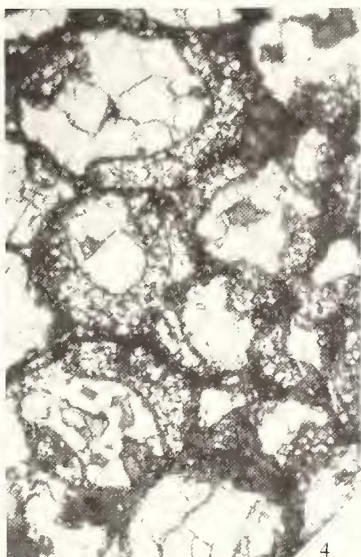
1



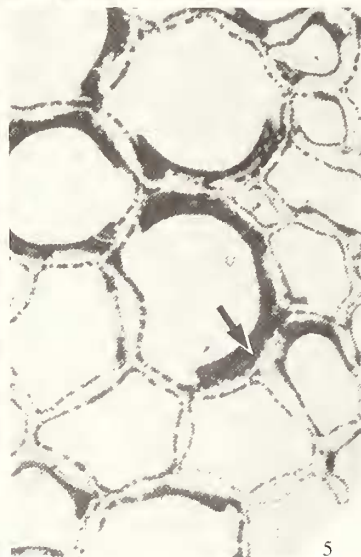
2



3



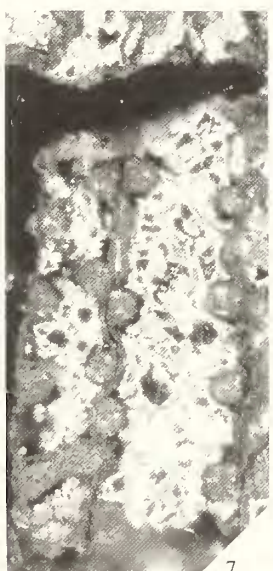
4



5



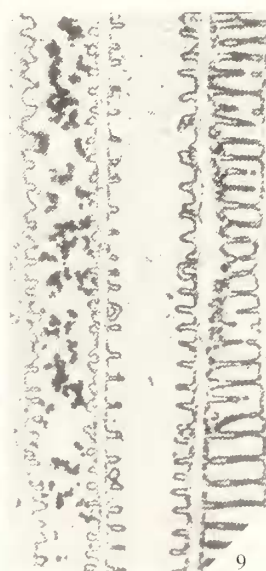
6



7



8



9



*Emended diagnosis.* Axes up to 6 mm diameter containing a terete xylem strand, 0.9–0.2 mm in cross-section. Xylem composed of elongate elements, with predominantly helical elements surrounding a clearly defined central region of narrower elements also helically thickened mixed with non-ornamented cells. Xylem element wall two layered: a thin continuous microporate layer (next to cell lumen) overlies a layer with a spongy texture. Micropores are 100 nm (40–200 nm) in diameter with a density of  $c. 16 \mu\text{m}^{-2}$ . Means and actual xylem measurements are as follows: width of thickening =  $11.2 \mu\text{m}$  (6.3–27.5  $\mu\text{m}$ ); inter-thickening distance =  $17.4 \mu\text{m}$  (5.0–32.5  $\mu\text{m}$ ); distance thickening protrudes into cell lumen =  $9.8 \mu\text{m}$  (5.0–13.8  $\mu\text{m}$ ); lumen diameter at widest point =  $34.5 \mu\text{m}$  (–45.0  $\mu\text{m}$ ); inter-thickening wall thickness  $c. 2.5 \mu\text{m}$ . Outer cortex composed of up to five layers of thick-walled ( $c. 5 \mu\text{m}$ ) cells, more or less isodiametric in cross-section but decreasing in diameter and length towards the outside; mean cell width =  $50 \mu\text{m}$  (25–100  $\mu\text{m}$ ) and cell length up to 450  $\mu\text{m}$ .

## DESCRIPTION OF ANATOMY

*Major features of the xylem.* The xylem is a more or less terete strand of elongate cells and in well preserved sections consists of two distinct zones. The outer zone is composed of large cells, up to six cells thick, and completely surrounds an inner zone of smaller cells. The boundary between the two zones is quite distinct (Pl. 1, figs 1 and 2; Text-fig. 1A). Preservation varies along a single axis and, in some regions, the central zone cells are not preserved. This appears to have resulted in collapse of the outer zone into the non-preserved central region and consequently a more elliptical outline to the strand (Text-fig. 1A).

*Outer zone xylem cells.* Each cell has a single large helical thickening with frequent reversals in the direction of the helix (see Table 1 for all measurements). The helical nature of the thickening is most clearly seen in etched transverse sections (Pl. 2, fig. 4); the reversal of the helix is most obvious in fractured lumen casts (Pl. 2, fig. 1). Cells are elongate, but no end walls were observed and so their total lengths are unknown. Variation in cell diameter within the outer zone suggests some tapering, but may merely indicate the presence of cells of different diameter (Pl. 2, fig. 1).

Scanning electron microscopy of fractured or etched sections shows the most ultrastructural detail (Pl. 2). At low magnification fractured sections commonly reveal lumen casts of coarse textured mineral with deep grooves marking the path of the helical thickening (Pl. 2, fig. 1: two cells on the left). Partially coalified cell walls are also present, have a smoother texture and usually retain the helical thickening itself (Pl. 2, fig. 1: two cells on the right). At higher magnification the wall is seen to consist of at least two layers: a very thin microporate layer overlies the bulk of the wall which has a spongy texture (Pl. 2, figs 2 and 3). The microporate layer is continuous over the entire inner surface of the cell and covers the thickenings as well as the wall between. Micropores, about

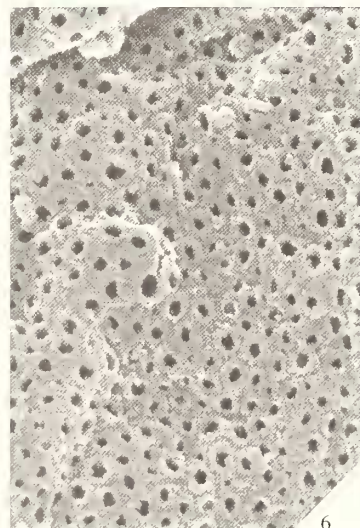
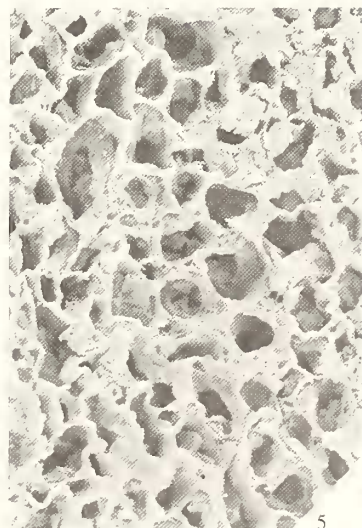
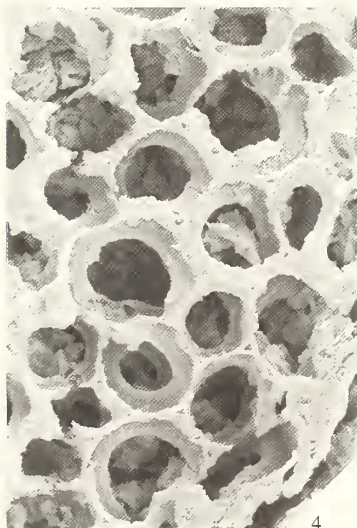
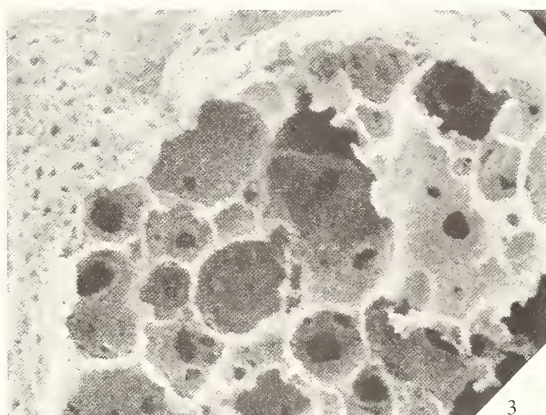
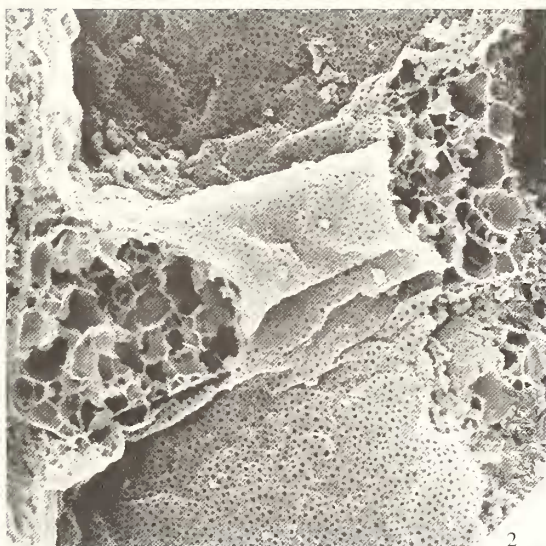
---

## EXPLANATION OF PLATE 2

Scanning electron micrographs of *Semicaulis*-type (S-type) xylem cell wall structure.

Figs 1–3, 6. NMW 90.42G.3, stub 183; Lower Old Red Sandstone; Mill Bay West, South Wales. 1, fractured and partially etched longitudinal section showing lumen casts of coarse textured mineral with deep grooves marking the path of the helical thickening (two cells on left) and coalified walls where lumen casts have fallen away with thickenings arrowed (two cells on right),  $\times 600$ . 2, higher magnification of area in figure 1 showing structure of wall thickening: microporate wall continuous over thickening and between thickenings,  $\times 3500$ . 3, details of spongy interior to thickenings,  $\times 12000$ . 6, details of microporate wall as seen from cell lumen,  $\times 14000$ .

Figs 4 and 5. NMW 85.18G.27f, stub 169; Siegenian; Brecon Beacons Quarry, South Wales; details of partially demineralized thickenings in outer and inner zone cells at the same magnification,  $\times 450$ . 4, outer zone cells, simple helical thickenings. 5, inner zone cells, some with helical thickenings.





100 nm in diameter (ranging between 200 nm to less than 40 nm diameter), penetrate this layer completely (Pl. 2, figs 2, 3, 6). The density of micropores is approximately  $16 \mu\text{m}^{-2}$ . The microporate layer is very thin; its actual thickness was difficult to measure but it is estimated as approximately equal to the micropore diameter of 100 nm or less. In all cells this layer is wrinkled and this is especially noticeable on and around the thickenings themselves (Pl. 2, figs 1 and 2). It should be noted that the small size of the micropores make them difficult to resolve even at high magnification. At low magnification the inner surface of the coalified wall appears to be smooth (compare Pl. 2, figs 1 and 2).

The remainder and bulk of the wall underlying the microporate layer has a distinctive appearance that is observed most easily within the helical thickening. It is a coalified layer with a spongy texture (Pl. 2, figs 2 and 3). A thinner layer of similar composition underlies the wall layer between thickenings. There appear to be no direct connections or channels through this spongy layer connecting the micropores of adjacent cells, nor any indication of a layer separating adjacent cells.

*Inner zone xylem cells.* This zone consists of helically thickened cells of similar structure to those in the outer zone but also contains cells without thickenings (Pl. 2, fig. 5). Thickened cells predominate and the nature of the unthickened cells is uncertain because of the paucity of well-preserved and uncompressed material within the inner region. All cells are distinctly smaller in diameter than those in the outer zone (compare Pl. 1, figs 1 and 2).

*Cellular preservation outside the xylem.* There is no cellular preservation outside the xylem in specimens from Mill Bay. However, specimens from the original Edwards collection of *Semicaulis hippocrepiformis* show a narrow zone of crushed cells immediately adjacent to the xylem and a further layer of cells close to or at the edge of the axis and separated from the central tissues by a region where there is no cellular preservation. A detailed analysis of cell wall structure in these regions has not yet been undertaken.

#### MINERALOGICAL OBSERVATIONS

All specimens considered here are preserved in pyrite, limonite, or a combination of both minerals. Limonite is used as a broad term that can encompass virtually any combination of the various iron oxides and hydroxides that exist naturally. In fossil plants it forms by the oxidation of pyrite and pseudomorphs pyrite textural morphologies. The timing of this oxidation cannot be defined more specifically than post pyrite formation.

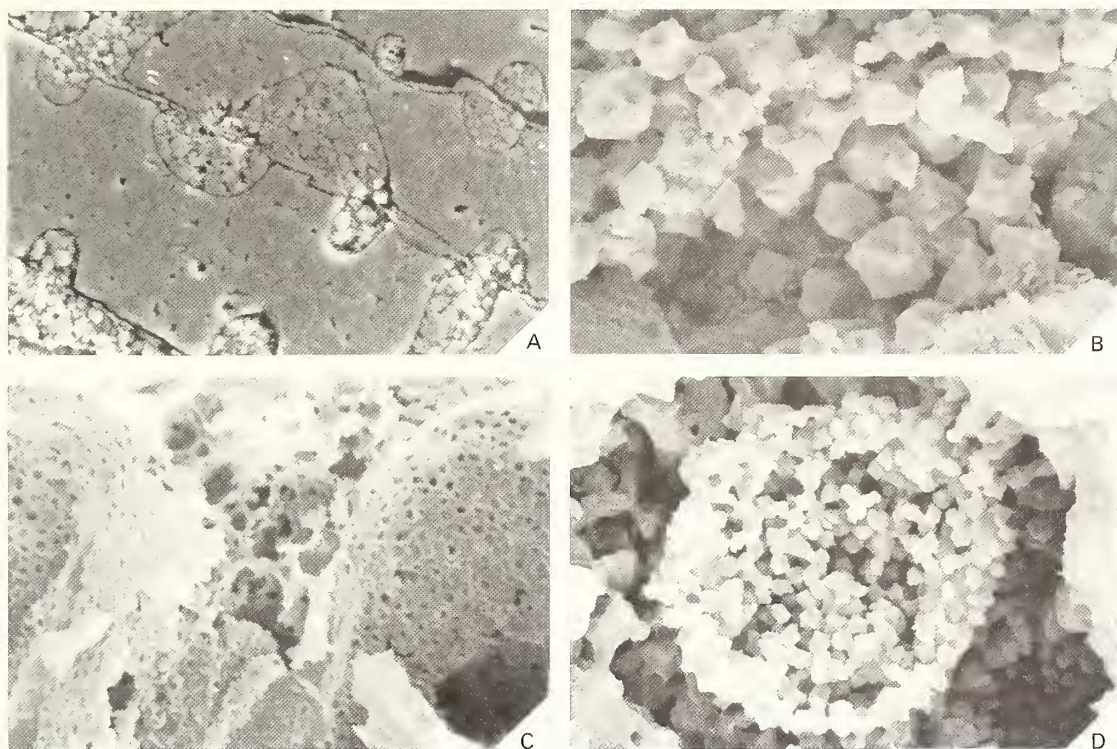
Observation of polished thick sections in reflected light clearly shows the distribution of mineral and coalified material in the wall of pyritized specimens (Pl. 1, figs 3 and 4), in that pyrite has high reflectance and the coalified material has low reflectance, although precise identification of coaly material in such sections remains a problem (Kenrick and Edwards 1988). While other non-opaque minerals (e.g. silicates) have a similar low reflectance, we interpret the spongy structure in the composite wall as organically derived, because it is acid resistant, has no discernible crystalline structure and is similar in composition and structure in all modes of permineralization in all occurrences. At very high magnifications both microporate and spongy material show a similar texture, which is not observed elsewhere in the permineralized cells.

##### *Pyrite textures*

Considering those in the lumen of the tracheid, pyrite textures can be divided into three morphologies.

*Equant euhedra of pyrite.* These have an average grain size of 4–10  $\mu\text{m}$  and are surrounded by a later overgrowth of pyrite. In transverse section 2–6 euhedra are visible in each cell lumen, while in longitudinal section many tens of euhedra were seen (Text-fig. 2A, B). Equant euhedra were also observed within the coalified helical thickenings (Text-fig. 2A).





TEXT-FIG. 2. Pyrite textures observed within the xylem of longitudinally fractured axes of *Semicaulis hippocrepiformis* from the Brecon Beacons Quarry, South Wales. A, V 60402; sections through pyrite euhedra in the helical thickenings following light etch,  $\times 1800$ . B, V 60402; euhedra within lumen: in such a deeply etched longitudinal section individual euhedra show their distinctive octohedral form,  $\times 2000$ . C, V 60415; strongly etched axis with helical thickenings (cf. Pl. 2, fig. 3) in which voids left by the removal of pyrite show little resemblance to the octohedral pyrite morphology, and are thought to be related to the original structure of the wall,  $\times 8280$ . D, V 60415; framboid within lumen of tracheid: individual crystallites  $\geq 1 \mu\text{m}$  cluster to form framboids 10–20  $\mu\text{m}$  diameter,  $\times 3450$ .

**Framboidal pyrite.** Framboids (Text-fig. 2D) are often surrounded by a later overgrowth or overgrowths of pyrite and are less common than in analogous areas of lumen in *Gosslingia breconensis* (Kenrick and Edwards 1988).

**Bladed pyrite.** Some pyrite crystals extend from points on or adjacent to the cell wall out into the cell lumen (Pl. 1, figs 1–4). Sometimes pyrite infilling of the cell lumen is incomplete, leaving a space which may be filled later with another diagenetic mineral, typically calcite (Pl. 1, figs 1–4).

The helical thickenings are filled with euhedra of pyrite (c. 2–4  $\mu\text{m}$ ) within what is interpreted as a coalified 'spongy' matrix. The high reflectance of the pyrite and the low reflectance of the coalified material give the 'C'-shaped thickenings a speckled appearance in polished section (Pl. 1, fig. 4, Text-fig. 2B).

In specimens that are partially pyritic and partially limonitic (Pl. 1, figs 1, 2, 7; Text-fig. 1A) particular care must be taken when interpreting the extent of the mineralization of the cell wall. Limonite formation in fossil plants generally seems to start within the cell wall and may or may not proceed to the pyrite of the lumen (Kenrick 1988). We suggest that the microcrystalline pyrite and

organic material within the wall provide a relatively easy route into the specimen for oxidizing chemicals. In contrast, the large pyrite crystals and paucity of coalified material within the cell lumen prove a more effective barrier to oxidation. Oxidation produces a mineral with reflectance similar to that of the coalified material but much lower than that of pyrite. This makes it difficult to assess the relative abundance and distribution of mineral within the cell wall of partially oxidized specimens using reflectance alone. Superficial examination may erroneously suggest (Pl. 1, figs 1, 2, 7) that the walls are heavily, or almost entirely, coalified.

Specimens in which most or all of the pyrite has been oxidized are better viewed in dark field illumination (Pl. 1, fig. 6; Text-fig. 1B). Although major wall features such as thickenings are easy to see, lack of contrast makes it difficult to assess the distribution of mineral and coalified material.

### TAPHONOMY

The description and interpretation of wall features in *Sennicaulis* in terms of original cell wall structures requires an understanding of taphonomic processes and an analysis of the effects of pyrite formation on cell wall structure. The process of sedimentary pyrite formation in recent sediments is relatively well understood (Berner 1984), and the way this process affects the appearance of the plant cell wall has been discussed at length by Kenrick and Edwards (1988) in relation to another Lower Devonian plant, *Gosslingia breconensis*.

The pyritization process in fossil plants is seen as one of selective decay by a consortium of bacteria ending with sulphate reducers and replacement by iron monosulphides which are eventually converted to pyrite. Decay of the fossil plant is selective because some tissue systems are less resistant to bacterial decomposition or more attractive in terms of energy yield than others. For example, woody tissue is persistent in the fossil record because of the decay-resistant lignin component within the cell wall, whereas thin-walled, non-lignified parenchyma is comparatively rarely preserved. Easily decomposed tissues may be entirely replaced by pyrite, whereas woody tissues often retain their original form although the organic material within the cell wall has been diagenetically altered. This argument has been extended to explain the distribution of pyrite and coalified material *within* a cell wall (Kenrick and Edwards 1988). For example, within the xylem cell walls of *Gosslingia breconensis* mineral and coalified material are distributed in a characteristic and consistent pattern. The most plausible explanation for this is that the distribution of coalified material faithfully reflects the pattern of decay resistant chemicals within the wall (usually identified as lignin) and the distribution of pyrite reflects the pattern of decay within the wall (i.e. the middle lamella and areas of cellulose with little or no aromatic components).

Mineral and coalified material are also distributed in a characteristic and consistent pattern in the cell wall of *Sennicaulis*, although in a different manner to that found in *Gosslingia*. Since there is little or no cellular preservation outside the xylem strand, the perforate coalified layer and the underlying spongy coalified material must be relatively decay resistant and therefore are interpreted as having an aromatic non-polysaccharide component. The microporate layer is of uniform composition and, by comparison to walls of similar outward appearance in the water-conducting cells of the Hepaticae, may be plasmodesmata derived, although their presence in the region of the thickenings is difficult to explain (see p. 764). The micropores are not preservation effects caused by microcrystalline pyrite growth because: (1) pyrite crystals of this size have not been observed in the cell wall, (2) the pores are not angular in outline as is the cubic crystal structure of the mineral, (3) the abundant larger pyrite crystals do not damage this layer, and (4) the feature is regular and uniform in plants from different localities. We also do not consider that the pores were produced during etching procedures as they are also present in fractured specimens. The wrinkling and thinness of the microporate layer suggests that, although resilient, its primary role was not structural. The underlying spongy layer that forms the bulk of the wall both within and between thickenings is more difficult to interpret. That it is decay resistant is evident; whether there was an entirely polysaccharide component occupying the cavities in the spongy texture or whether those cavities were water or air-filled features of the wall is difficult to assess. It seems unlikely that the

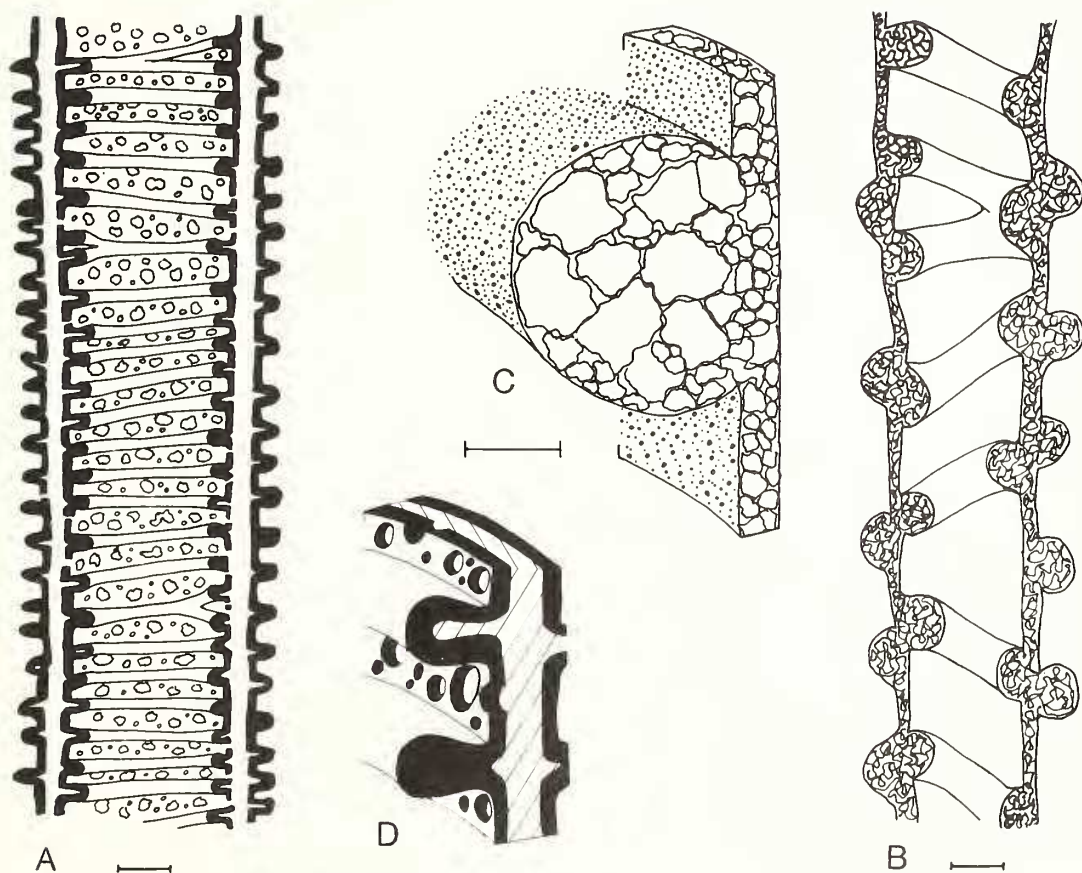


spongy texture is an artefact caused by pyrite crystal growth within the cell wall because the shape of the cavities does not mirror the cubic crystal structure of the mineral.

### TERMINOLOGY AND COMPARISONS OF CONDUCTING ELEMENTS

We propose the terms 'S-type' and 'G-type' for the types of wall thickening and composition in two distinctive early land plant water-conducting cells (Text-fig. 3).

The 'S-type' as exemplified by *Sennicaulis* is an elongate cell with a large, simple helical thickening (*sensu* Bierhorst 1960). The wall is two layered: a thin, continuous, coalified, microporate inner layer (next to the cell lumen) overlies a thick coalified spongy layer forming most of the



TEXT-FIG 3. Diagrammatic representation of G-type (*Gosslingia*) (A, D) and S-type (*Sennicaulis*) (B, C) cells and cell walls. A, B, longitudinal sections through G-type and S-type cells at the same magnification, showing in face view the shape, size and density of the thickenings; scale bar = 10  $\mu\text{m}$ ; A, G-type note the discontinuous nature of the inner wall layer (i.e. that part of the wall facing the lumen); B, S-type note the continuous wall over and between thickenings. C, D, S-type and G-type cell walls in section at the same magnification; scale bar = 2  $\mu\text{m}$ ; C, S-type showing two layered wall the bulk of which is made from a spongy material underlain by the very thin microporate wall (stippled). Stippling indicates size and density of micropores on surface and is not for purposes of shading; D, G-type showing two layered wall: an inner decay-resistant layer (black in section, white on the surface) and an outer layer not resistant to decay often also found inside thickenings (shaded with diagonal lines).

interior of the thickening and the wall between thickenings. The coalified remains represent relatively decay resistant material within the cell wall, but their distinctive form and distribution are unlike that seen in the lignified walls of tracheids. Since we can find no comparable structures in tracheids of extant plants, except for the helical thickening, we consider it unwise to go further and interpret the original chemical composition of the decay resistant component as 'lignin', although presumably it is of an aromatic nature.

The 'G-type' is typified by *Gosslingia breconensis* (Kenrick and Edwards 1988) and has indirectly attached annular or tilted annular thickenings (*sensu* Bierhorst 1960). In fossils the indirect attachments are in the form of perforated sheets of coalified material between adjacent annular bars. Some elements also have direct attachment between adjacent annular bars (*sensu* Bierhorst 1960). In pyrite permineralizations the wall is clearly two layered: a relatively thick discontinuous coalified layer overlies one replaced by pyrite. The distribution of pyrite reflects the distribution of decay resistant chemicals within the cell wall (Kenrick and Edwards 1988) and since this pattern in the G-type is similar to that in the tracheids of some extant plants, we tentatively interpret the chemical composition of the decay resistant component as 'lignin', and the pyritized one as predominantly cellulose.

In polished longitudinal section both types of cell appear superficially similar as it is impossible to distinguish unequivocally between helical and tilted annular thickenings. However, direct comparison at the same magnification shows several obvious differences in the size, shape and distribution of thickenings (compare S-type element in Plate 1, figs 6 and 7, with G-type element in Plate 1, figs 8 and 9; Table 1). The S-type elements have larger thickenings that are more rounded and widely spaced, even though cell lumen diameters in both types of cell are very similar. Taking mean values, thickenings in the S-type element are three times as large and six times further apart than those in G-type elements of comparable lumen diameter. An interesting result is that in cells of comparable maximum lumen diameter, the effective diameter for fluid conductance (Jeje and Zimmermann 1979) in the S-type cell is just over half what it is in the G-type (Table 1). This is most noticeable in transverse sections of similar magnification viewed side by side (compare S-type element in Plate 1, fig. 4 with G-type element in Plate 1, fig. 5; Table 1).

TABLE 1. Comparative measurements of cell wall dimensions for S-type and G-type cells. For fuller explanation of  $\delta$ ,  $\Sigma$ ,  $t$ ,  $W$ ,  $D$  and  $TW$  see Kenrick and Edwards (1988).  $\delta$  = width of thickening;  $\Sigma$  = interthickening distance;  $t$  = distance thickening protrudes into cell lumen;  $W$  = maximum lumen diameter;  $D$  = effective diameter for fluid conductance;  $TW$  = thickness of wall. MBW = Mill Bay West, BBQ = Brecon Beacon Quarry, N = number of measurements.

Element type	Locality		$\delta$	$\Sigma$	$t$	$W$	$D$	$TW$
S-type	MBW	mean $\mu\text{m}$	11.2	17.4	9.8	34.5	14.9	2.5
		max. $\mu\text{m}$	27.5	32.5	13.8	45.0	17.4	—
		min. $\mu\text{m}$	6.3	5.0	5.0	—	—	—
		N	74	77	52	11	—	—
G-type	BBQ	mean $\mu\text{m}$	3.3	2.8	3.6	29.6	22.4	—
		max. $\mu\text{m}$	4.5	5.3	6.1	50.0	37.8	3.5
		min. $\mu\text{m}$	1.5	1.0	1.5	—	—	1.5
		N	36	33	16	23	—	—

Only helical thickenings were observed in the S-type element (clearly seen in scanning electron micrographs of etched sections, Pl. 2, fig. 4). The frequent reversal in direction of the helix in the S-type cell (Pl. 2, fig. 1) has also not been seen in the G-type. Both annular and helical thickenings clearly occur in the G-type element along with frequent direct connections between adjacent annular bars.



Ultrastructural differences are still more marked (Text-fig. 3). Both types of cell have a wall of at least two layers although whether or not homologous is debatable. In the S-type cell, the inner part of the wall is preserved as a very thin, coalified, microporate layer that is continuous over the entire inner surface of the cell. In the G-type cell, the inner part of the wall is relatively thick and continuous over the inner surface of the cell except for relatively large holes of variable size between thickenings (see Text-fig. 3). Unlike the micropores in the S-type element, these holes never occur on the thickenings themselves. The micropores of the S-type element are about 100 nm diameter (ranging from 200 nm to less than 40 nm) with a density of about  $16 \mu\text{m}^{-2}$ , whereas the holes in the G-type measure about 2–3  $\mu\text{m}$  diameter (ranging from 4  $\mu\text{m}$  to about 0.5  $\mu\text{m}$ ).

The second layer or outer part of the wall in the G-type element which is entirely pyritized in *Gosslingia* is approximately the same thickness as the inner. In contrast, the outer layer of the S-type element forms the bulk of the wall and although partially pyritized contains a significant proportion of structured coalified material (Text-fig. 2c).

### DISTRIBUTION OF S- AND G-TYPES

#### *S-type*

There is only one other fossil plant in which ultrastructural features comparable to those in the S-type element have been described. Hueber (1982) described helically strengthened tubes in axes assignable to *Taeniocrada dubia*. He observed three components in the structure of the wall: 'an outer, thin, fibrillar layer; sponge-textured helical thickenings; and a microporate layer that lines the lumen of the tube'. Apart from the outer, thin, fibrillar layer which has not been observed in S-type elements from *Sennicaulis* the structure of the wall would appear to be identical although no photographs of Hueber's material have yet been published. The conducting strand is described as centrarch in *T. dubia* but in *Sennicaulis* from the Mill Bay locality it is clearly divided into two distinct zones, at least over part of the axis. The inner zone is often not well preserved and in many sections is totally missing. When this occurs, the outer zone cells collapse inward and this, combined with the presence of crushed cells in the centre, may give the impression of a centrarch strand.

Few ultrastructural studies have been performed on early land plant water-conducting cells so it is impossible to identify unequivocally other plants with similar wall structure. However, the shape and size of the helical thickenings in the S-type cell are strikingly different from those in the G-type (see Table 1 and p. 761) and may prove to be characteristic. The recent reinvestigation of *Stockmansella langii* (formerly *Taeniocrada langii*) illustrates cells with certain similarities to the S-type (Fairon-Demaret 1985, 1986), although organic material in the cell wall could not be recognized. Fairon-Demaret (1985) noted that the spacing and tilt of the thickenings, seen as grooves on goethite casts of the cell lumen, indicate a simple helical thickening with frequent inversions in the tilt, and that in this feature these cells are similar to those of *Rhynia gwynne-vaughanii*. These features, together with the dimensions of the thickening, point to a structure similar to that in the S-type cell.

Edwards (1981) and Edwards, D. S. (1986) have both commented on the similarities between the helical elements of *Sennicaulis hippocrepiformis* and *Rhynia gwynne-vaughanii*, including the size and shape of thickenings, originally described as annular in *R. gwynne-vaughanii* (Kidston and Lang 1917), and the frequent reversal of the helix within cells, all typical features of the S-type element. Edwards D. S. (1986) was unable to find an organic wall in etched tracheids of *R. gwynne-vaughanii*, so the wall ultrastructure is unknown. The xylem strand of *R. gwynne-vaughanii* is also much smaller than that illustrated here and is not divided into distinct zones.

There are no known examples of S-type conducting cells among extant vascular plants. Helical elements are common in the protoxylem, but lignin never forms in a continuous sheet on the inner surface of the cell, nor are there micropores comparable to those illustrated here.

Although the microporate layer is unknown in tracheids, a wall of similar appearance, but lacking helical thickenings and, presumably, decay resistant aromatics, is sometimes found in bryophyte

gametophytes (Héban 1979). In certain Hepaticae, as well as the enigmatic genus *Takakia*, the presumed cellulose walls of water-conducting cells have numerous plasmodesmata-derived perforations of similar size and density to those found in *Sennicaulis*. (Compare Plate 2, figures 2 and 6 with Héban's (1979) figure 2.) The whole wall thickness of these cells is similar to the thickness of the microporate layer in the S-type element. Such a microporate wall is not found in the hydroids of mosses (Héban 1979).

### G-type

A review of the distribution of G-type elements was given by Kenrick and Edwards (1988). Earlier reports of scalariform or reticulate pitting in zosterophylls have been shown to be incorrect in all instances where scanning electron microscopy has been undertaken. Instead, G-type elements with annular or helical thickenings characterize the metaxylem of zosterophylls, Barinophytales and a group of fossil plants (*Asteroxylon*, *Baragwanathia* and *Drepanophycus*) similar in vegetative characteristics to modern herbaceous lycopods. With one exception (*Leclercqia*, Grierson 1976), the protoxylem elements of those and other important Devonian taxa have not received the same detailed consideration as the metaxylem and are described as helical or annular.

## GENERAL DISCUSSION

In our studies of *Gosslingia* tracheids we were able to interpret their wall structure in terms of that in extant tracheids, although examples are rare. In addition it is possible that the perforate sheet in the G-type element is homologous with the pits of trimerophytes where there are perforated sheets of secondary wall material within the pit chamber (Hartman and Banks 1980) and possibly even with strands of secondary wall material in the pits of Carboniferous lycopods.

In contrast to all these taxa, the gross morphology of the plants that produced S-type cells is poorly understood and the structure cannot be directly related to other presumed water-conducting cells. Compression fossils of *Sennicaulis hippocrepiformis* from Brecon Beacons Quarry are unknown but permineralizations suggest that the axes were more or less terete in cross section. The Mill Bay West anatomy was obtained from compressions of long, ribbon-like, sterile axes. The Gaspé (Quebec) specimens of *Taeniocrada dubia*, which show a similar cell-wall structure, were originally described by Dawson as the rhizomata of *Psilophyton princeps* (Hueber 1967, 1982). Hueber (1982) described the plant as ribbon-like, with a thin cuticle and stomata. Reproductive parts were not found on specimens from which he isolated anatomy, although terminal sporangial trusses have been described from German material (Høeg 1967; Kräusel and Weyland 1930).

Gross morphology is better understood in *Stockmansella langii* (Fairon-Demaret 1985, 1986) and *Rhynia gwynne-vaughanii* (Edwards D. S. 1986), taxa united by sporangial abscission. Ultrastructural wall features have not been described for either plant and are currently under investigation.

The novel wall structure in the water-conducting cells of *Sennicaulis* and *Taeniocrada* cannot easily be compared with that in extant tracheids nor indeed with hydroids in mosses. The cell is superficially similar to an early formed protoxylem tracheid in that it has a helical thickening, but the wall layers are unlike those in the tracheids of extant plants and the more tracheid-like cells of some early land plant fossils. Terms such as primary and secondary wall are difficult to apply and have been avoided. The micropores are probably developmentally similar to the plasmodesmata derived pores in the water-conducting cells of some hepatics and functionally similar, at least in the wall layer between thickenings, but their presence in the layer over the latter is more difficult to interpret developmentally. The cell might be considered plesiomorphic in this respect.

Reinvestigation of the cell walls of the xylem of *Rhynia major*, now *Aglaophyton major*, showed that there are no internal thickenings and that the plant does not have tracheids (D. S. Edwards 1986). This was a surprising find in one of the two species of a genus that has come to represent the archetypal early vascular plant, and demonstrates that branched sporophytes do not imply vascular plant status. Our investigation shows that helical thickenings in water-conducting cells do not imply



a tracheid-like wall structure. In the case of *Semicaulis*, ultrastructural studies were required to demonstrate the novel organization. Many early land plant fossils of the rhyniophyte grade are included in Tracheophyta because of helical or annular thickenings in the xylem cells. The systematic position of these fossils must be re-evaluated because in most cases detailed studies of water-conducting cells have not been undertaken. It is natural to go further and question whether 'tracheid' can be used as a synapomorphy for vascular plants and to speculate on the relationships of plants with S-type cells. For the moment we do not wish to go beyond the recognition of a level of organization that would seem to fall between that of the extant bryophytes and vascular plants. More information is required on the morphology of plants with S-type cells and an exhaustive phylogenetic analysis is necessary before explicit statements of relationships can be made.

*Acknowledgements.* Paul Kenrick was financed by NERC research grant No GR3/5069 and a grant from the Field Museum of Natural History, and Robin Dales by a NERC postgraduate research studentship. All sources of funding are gratefully acknowledged. P. K. acknowledges the helpful criticism of Peter Crane and Andrew Drinnan.

## REFERENCES

- ALLEN, J. R. L. 1974. The Devonian rocks of Wales and the Welsh Borderland. 47–84. In OWEN, T. R. (ed.). *The Upper Palaeozoic and post-Palaeozoic rocks of Wales*. University of Wales Press, Cardiff.
- BERNER, R. A. 1984. Sedimentary pyrite formation: an update. *Geochimica et Cosmochimica Acta*, **48**, 605–615.
- BIERHORST, D. W. 1960. Observations on tracheary elements. *Phytomorphology*, **10**, 249–305.
- BIGGS, D. L. and ROCKEN, R. J. 1983. Paragenesis of iron sulfide as a function of coal rank. *Tenth International Congress on Carboniferous Stratigraphy and Geology*, **3**, 145–164.
- EDWARDS, D. 1981. Studies on Lower Devonian petrifications from Britain 2. *Semicaulis*, a new form genus for sterile axes based on pyrite and limonite petrifications from the Senni Beds. *Review of Palaeobotany and Palynology*, **32**, 207–226.
- and KENRICK, P. 1986. A new zosterophyll from the Lower Devonian of Wales. *Botanical Journal of the Linnean Society of London*, **92**, 269–283.
- EDWARDS, D. S. 1986. *Aglaophyton major*, a non-vascular land-plant from the Devonian Rhynie Chert. *Botanical Journal of the Linnean Society of London*, **93**, 173–204.
- FAIRON-DEMARET, M. 1985. Les plantes fossiles de l'Emsien du Sart Tilman, Belgique. 1. *Stockmansia langii* (Stockmans) *comb. nov.* *Review of Palaeobotany and Palynology*, **44**, 243–260.
- 1986. *Stockmansella*, a new name for *Stockmansia* Fairon-Demaret (fossil). *Taxon*, **35**, 334.
- FRIEND, P. F. and WILLIAMS, B. P. J. (eds). 1978. A field guide to selected outcrop areas of the Devonian of Scotland, the Welsh Borderland and South Wales. *International Symposium on the Devonian System (P.A.D.S. 78)*. The Palaeontological Association, London, 106 pp.
- GRIERSON, J. D. 1976. *Leclercqia complexa* (Lycopside, Middle Devonian): its anatomy, and the interpretation of pyrite petrifications. *American Journal of Botany*, **63**, 1184–1202.
- HARTMAN, C. M. and BANKS, H. P. 1980. Pitting in *Psilophyton dawsonii*, an early Devonian trimerophyte. *American Journal of Botany*, **67**, 400–412.
- HÉBANT, C. 1979. Conducting tissues in bryophyte systematics. 365–383. In CLARKE, G. C. S. and DUCKETT, J. G. (eds). *Bryophyte systematics: Systematics Association special volume 14*. Academic Press, London and New York.
- HOEG, O. A. 1967. Psilophyta. 191–352. In BOUREAU, E. (ed.). *Traité de Paléobotanique*. II. Masson et Cie, Paris.
- HUEBER, F. M. 1967. *Psilophyton*: the genus and the concept. 815–822. In OSWALD, D. H. (ed.). *International symposium on the Devonian System 2*. Alberta Society of Petroleum Geologists, Calgary.
- 1982. *Taeniocrada dubia* Kr. and W.: its conducting strand of helically strengthened tubes. *Botanical Society of America, Miscellaneous Series (Abstract)*, **162**, 58–59.
- JEJE, A. A. and ZIMMERMANN, M. H. 1979. Resistance to water flow in xylem vessels. *Journal of Experimental Botany*, **30**, 817–827.
- KENRICK, P. 1988. Studies on Lower Devonian plants from South Wales. Unpublished Ph.D. thesis, University of Wales, Cardiff.

- KENRICK, P. and EDWARDS, D. 1988. The anatomy of Lower Devonian *Gosslingia breconensis* Heard based on pyritized axes, with some comments on the permineralization process. *Botanical Journal of the Linnean Society*, **97**, 95–123.
- KIDSTON, R. and LANG, W. H. 1917. On Old Red Sandstone plants showing structure, from the Rhynie Chert Bed, Aberdeenshire. Part I. *Rhynia gwynne-vaughani* Kidston and Lang. *Transactions of the Royal Society of Edinburgh*, **51**, 761–784.
- KRÄUSEL, R. and WEYLAND, H. 1930. Die Flora des deutschen Unterdevons. *Abhandlungen der Preussischen geologischen Landesanstalt, Berlin*, **131**, 1–92.
- RICHARDSON, J. B., STREEL, M., HASSAN, A. and STEEMANS, Ph. 1982. A new spore assemblage to correlate between the Breconian (British Isles) and the Gedinian (Belgium). *Annales de la Société Géologique de Belgique*, **105**, 135–143.
- THOMAS, R. G. 1978. The stratigraphy, palynology and sedimentology of the Lower Old Red Sandstone Cosheston Group, S. W. Dyfed, Wales. Unpublished Ph.D. thesis, University of Bristol.

P. KENRICK

Department of Geology  
Field Museum of Natural History  
Roosevelt Road at Lake Shore Drive  
Chicago, Illinois 60605, USA

D. EDWARDS and R. C. DALES

Department of Geology  
University of Wales College of Cardiff  
P.O. Box 914, Cardiff CF1 3YE, UK

Typescript received 20 September 1990

Revised typescript received 28 November 1990